Acta Oceanol. Sin., 2021, Vol. 40, No. 1, P. 4–12
https://doi.org/10.1007/s13131-021-1719-0
http://www.hyxb.org.cn
E-mail: hyxbe@263.net

Evaluation of vertical crustal movements and sea level changes around Greenland from GPS and tide gauge observations

Jiachun An[1], Baojun Zhang[1, 2*], Songtao Ai[1*], Zemin Wang[1], Yu Feng[1, 3]

[1] Chinese Antarctic Center of Surveying and Mapping, Wuhan University, Wuhan 430079, China

[2] State Key Laboratory of Information Engineering in Surveying, Mapping and Remote Sensing, Wuhan University, Wuhan 430079, China

[3] Department of Brewing Engineering, Moutai Institute, Renhuai 564507, China

Received 27 August 2020; accepted 29 September 2020

Abstract

To better monitor the vertical crustal movements and sea level changes around Greenland, multiple data sources were used in this paper, including global positioning system (GPS), tide gauge, satellite gravimetry, satellite altimetry, glacial isostatic adjustment (GIA). First, the observations of more than 50 GPS stations from the international GNSS service (IGS) and Greenland network (GNET) in 2007–2018 were processed and the common mode error (CME) was eliminated with using the principal component analysis (PCA). The results show that all GPS stations show an uplift trend and the stations in southern Greenland have a higher vertical speed. Second, by deducting the influence of GIA, the impact of current GrIS mass changes on GPS stations was analysed, and the GIA-corrected vertical velocity of the GPS is in good agreement with the vertical velocity obtained by gravity recovery and climate experiment (GRACE). Third, the absolute sea level change around Greenland at 4 gauge stations was obtained by combining relative sea level derived from tide gauge observations and crustal uplift rates derived from GPS observations, and was validated by sea level products of satellite altimetry. The results show that although the mass loss of GrIS can cause considerable global sea level rise, eustatic movements along the coasts of Greenland are quite complex under different mechanisms of sea level changes.

Key words: Greenland ice sheet, GPS, vertical crustal movement, tide gauge, sea level change

Citation: An Jiachun, Zhang Baojun, Ai Songtao, Wang Zemin, Feng Yu. 2021. Evaluation of vertical crustal movements and sea level changes around Greenland from GPS and tide gauge observations. Acta Oceanologica Sinica, 40(1): 4–12, doi: 10.1007/s13131-021-1719-0

1 Introduction

The Greenland ice sheet (GrIS) accounts for approximately 10% of the total ice over the world, and if the GrIS ablated completely, the global sea level would rise by approximately 6.5 m (Chen et al., 2006). Therefore, it is of great significance to study the variations in the Greenland ice sheet and its effects on vertical crustal movements and sea level change.

The global positioning system (GPS) technique can provide continuous monitoring of the vertical velocity field and the mass balance in Greenland. However, due to the small number of stations in Greenland before 2010, most research focused on individual stations at that time. Wahr et al. (2001) analysed the uplift rates over the period of 1995–2001 using two GPS stations in southern Greenland and the speed of GPS is significantly different from the estimated speed of the glacial isostatic adjustment (GIA) model. Khan et al. (2007) processed the observations of five GPS stations in Greenland and estimated the contribution of the two nearby glaciers (Helheim Glacier and Kangerdlugssuaq Glacier) using a digital elevation model (DEM), who found that the remaining uplift was attributed to the loss of glacial mass near the southeast coast. Khan et al. (2008) validated the applicability of the ICE-5G model using data from seven GPS stations and a tide gauge station and found that the model overestimates the subsidence rate of these stations. In 2007, the Technical University of Denmark (DTU) teamed up with Ohio State University (OSU) to deploy more than 40 GPS stations in the coastal area of Greenland to form the Greenland network (GNET), which promotes increasingly comprehensive study of the Greenland ice sheet. Bevis et al. (2012) processed observations from GNET and pointed out that all sites showed an uplift trend, and in the summer of 2010, the rate of uplift increased significantly, which was highly related to the abnormal mass loss during that particular year. At the same time, the digital climate model and gravity recovery and climate experiment (GRACE) data are used to explore the seasonal variations of GPS time series, by analysing the effects of ice mass variations, climate cycles and climate change (Bevis et al., 2012). Based on the coordinate time series of 18 GNET stations and observations of atmosphere and sea temperature, Yang et al. (2013) also inferred that there was an uplift anomaly in southern Greenland in 2010, and the ablation of snow and ice was closely related to the change in subsurface water temperature. Khan et al. (2016) used GNET data to re-evaluate the impact of GIA since the last glacial period, and the results show that the maximum uplift rate caused by GIA in the southeastern region is up to 12 mm/a. Liu et al. (2017) processed the data of two GPS stations on the west coast of Greenland and found the atmospheric pressure, ocean bottom pressure, continental water storage and surface mass balance model can quantify

Foundation item: The National Key R&D Program of China under contract No. 2016YFC1402701; the National Natural Science Foundation of China under contract Nos 41941010, 41531069 and 41476162.
*Corresponding author, E-mail: bjzhang@whu.edu.cn; ast@whu.edu.cn

the contribution of various factors to the periodic term. However, in GPS data processing, time-dependent noise and location-dependent noise could be considered further to improve time series of GPS coordinates. In regard to time series of GPS coordinates, the noise in the time series is time-dependent rather than white noise (Mao et al., 1999; Williams et al., 2004; Zhang et al., 1997).

The sea level around Greenland has been investigated by tide gauges (Richter et al., 2011; Spada et al., 2014), laser altimetry (Spada et al., 2012), radar altimetry (Cheng et al., 2015; Rose et al., 2019), and satellite gravity (Brunnabend et al., 2015; Forsberg et al., 2017; Li et al., 2013). With a 1991–2015 average annual mass loss of 0.47 mm sea level equivalent (SLE) and a peak contribution of 1.2 mm SLE in 2012, the GrIS has recently become a major source of global mean sea level rise (van den Broeke et al., 2016). A sea level rise of 1.54 mm/a in Arctic Ocean is found in the total time period from 1991 to 2018 by using from four ESA radar altimeter satellites (Rose et al., 2019). However, the tide gauge records are still more accurate for sea level estimation locally than satellite-based observations, despite the unsatisfactory numbers and distribution of Greenland tide gauges.

Based on the above analysis, this paper uses the observations of more than 50 GPS stations and 4 tide gauge stations for the 2007–2018 period to analyse the vertical crustal movements and sea level changes around Greenland. For more accurate time series of GPS coordinates, the coloured noises are separated, and the common mode error (CME) is eliminated with principal component analysis (PCA). The impact of mass anomaly changes on stations and the response of stations to current mass changes in ice and snow are investigated using the GIA model and GRACE observations. The absolute sea level around Greenland was analysed by combining the relative sea level derived from tide gauge observations and the crustal uplift rates derived from GPS observations, and altimetry-based sea level products were used to validate tide gauge-based sea level estimation.

2 Data and methods

2.1 *GPS data and processing*

Figure 1 shows the GPS stations used in this paper. There are four GPS stations of the International GNSS Service (IGS) in Greenland, of which three are on the west coast, including THU3, KELY and QAQ1, and only one station, SCOR, is on the east coast. The IGS stations around Greenland include ALRT, QIKI, and NAIN in Canada, REYK and HOFN in Iceland and NYAL and TRO1 in Norway. The 11 IGS stations form the core framework of the GPS data processing. In 2007, DTU and OSU started the GNET, with more than 40 GPS stations in the coastal area of Greenland. In this paper, 42 GNET GPS stations are collected from UNAVCO. All the stations are situated on bedrock.

The GPS observations were processed using GAMIT/GLOBK

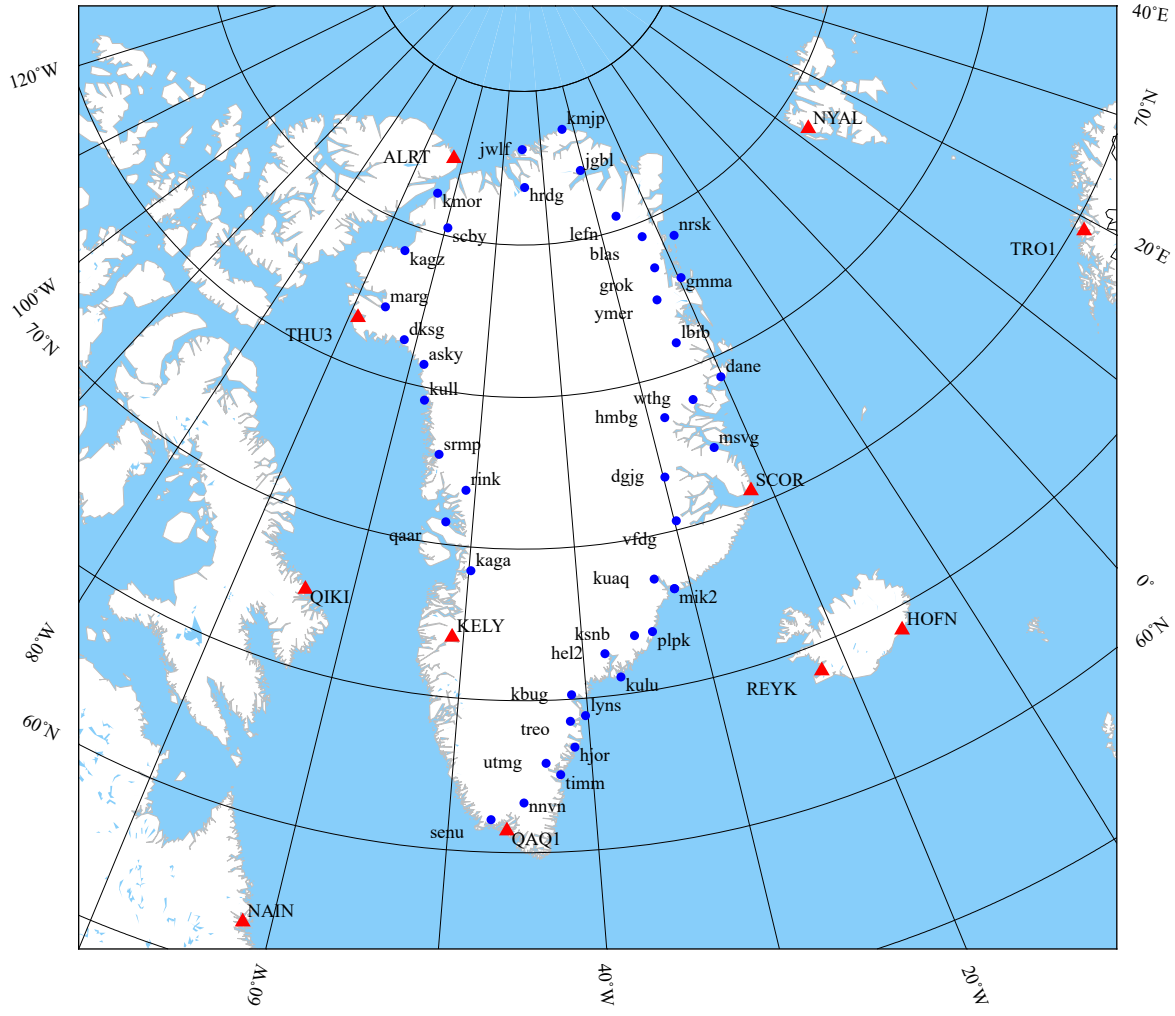

Fig. 1. IGS and GNET site map in and around Greenland (red triangles represent IGS stations, and blue dots represent GNET stations).

10.6 (Herring et al., 2015). The main solution strategy is outlined as follows: Broadcast ephemeris and sp3 precise ephemeris are provided by IGS, and observations of free ionospheric combination were used after automatic cycle slip repair mode (LC_AUTCLN). The satellite cut off elevation angle is 15°, and the sampling interval is 30 s. The tropospheric delay model is the Saastamoinen model, and the ionospheric constraint is 0.0 mm+8.00 ppm. Optical pressure perturbation correction is completed with the BERNE model, and tidal correction is completed with the FES2004 model. The fixed IGS station coordinate constraints are 0.05 m, 0.05 m, and 0.10 m, and the remaining station coordinate constraints are 100 m, 100 m, and 100 m. In addition, the relaxation solution (RELAX) is performed by solving the satellite orbital parameters at the same time. After baseline processing, GLOBK is used to perform network adjustment under the ITRF2008 framework. Since the stations used in this paper are in a regional GPS network, to maintain the stability of the framework, 91 core stations in IGb08 are selected as the framework stations. The station coordinates (north, east, up) are each given a constraint of 10 m. UT1 and the pole positions are given relaxation constraints. The daily h-files of 9 global subnets in 2007–2018 from Scripps orbit and permanent array center (SOPAC) are added to adjust the IGS global network baseline solution. For some GPS stations that changed suddenly due to earthquake or antenna changes, itrf08_comb.eq is used to rename these stations and to obtain the daily station coordinate time series of these stations.

In this paper, CATS software (Williams et al., 2004) is used to estimate the vertical velocity field of the GPS station under the consideration of two kinds of coloured noises, flicker noise and random walk noise. The outliers are eliminated by using the interquartile range (IQR). The error in the daily solution of the GPS station is caused by different noises, some of which are station-dependent, and some are location-dependent. The location-dependent noise can be caused by satellite orbit error and reference frame error and is usually called CME (King et al., 2010). In this paper, PCA is used to identify the principal components in the spatial distribution of the CME. The normalized principal component and its corresponding normalized eigenvalues are calculated by the method proposed by Dong et al. (2006).

2.2 *GRACE data and processing*

As a mission that observes earth's gravitational field, GRACE consists of two identical satellites that fly about 220 km apart in a polar orbit 500 km above the Earth, operated by the National Aeronautics and Space Administration (NASA) and the German Aerospace Center (DLR). The Jet Propulsion Laboratory (JPL), the Center for Space Research (CSR), the University of Texas at Austin (UTCSR) and the Potsdam Geoscience Center (GFZ) are responsible for GRACE data processing and archiving. The time-varying gravitational field observed by GRACE can be used to estimate the redistribution of earth mass, such as changes in the atmosphere, oceans, and groundwater (Tapley et al., 2004). In this paper, we use the RL05 version of the global gravity anomaly grid data (Monthly Mass Grids-Global mascons) provided by JPL to calculate the response of GPS stations to mass changes. The data are properly processed using the C20 coefficient from laser satellite ranging (SLR) to replace the C20 coefficient of GRACE (Cheng et al., 2013) by estimating the geocentric correction (Swenson et al., 2008) and correcting the GIA (Geruo et al., 2012). In addition, the datasets are processed by using the coastline resolution improvement (CRI) filter to separate the influences of sea and land (van Dam et al., 2007).

2.3 *Tide gauge data and processing*

Tide gauges usually measure the sea level relative to a nearby geodetic benchmark. Once the influence of the local vertical land motion is eliminated, tide gauge measurements can be used to estimate absolute sea level. Four tide gauge stations around Greenland are used in this paper, including NUUK, QAQO, SCOR and THUL, which are provided by the Technical University of Denmark (DTU). The time span of the collected tidal observations is generally consistent with that of the GPS stations. After eliminating outliers in tide gauge records and deriving relative sea level change at tide gauge stations, the absolute sea level can be further obtained by combining relative sea level and crustal uplift rates derived from GPS observations. In addition, global altimetric sea level anomaly products were used to further analyse the sea level change around Greenland, which was given with monthly grids by archiving, validation and interpretation of satellite oceanographic data (AVISO). To better validate the sea level from tide gauge observations, the local sea levels of AVISO were interpolated to the locations of tide gauges. Although the presence of sea ice can limit the use of altimetry to some extent, the reliability of altimetry on sea level estimation in Arctic region with coverage up to 82°N was verified adequately (Cheng et al., 2015; Rose et al., 2019).

3 Results and discussion

3.1 *Performance of PCA filtering*

Figure 2 shows the cumulative contribution rate of principal component (PC) eigenvalues, where the horizontal axis denotes the order of PCs and the vertical axis represents the percentage of the cumulative contribution rate of principal component eigenvalues. If we arrange the eigenvectors so that the eigenvalues are in descending order, the first few PCs represent the biggest contributors to the variance of the network residual time series, usually related to the common source time function (Dong et al., 2006). As shown in Fig. 2, the cumulative contribution rate of the first three principal components obtained by the PCA method is 67.11%, and the higher-order PCs are much less than the first few PCs, usually related to local or individual site effects.

The filtered results are obtained by subtracting the corresponding common mode error from the coordinate time series and the residual time series. To quantify the influence of the common mode error derived from PCA on the time series of the station coordinates, Table 1 shows the variations in standard deviations (stds) of residuals before and after filtering. After subtracting the common mode error, the stds of the residuals of all stations are reduced significantly, which indicates the good performance of the PCA.

3.2 *Vertical velocity derived from GPS stations*

Figure 3 shows the vertical velocity field of stations estimated using CATS software. As shown in Fig. 3, all stations in the coastal area of Greenland rise. The stations near the outlet glacier have higher speeds, such as HEL2 near Helheim (HH), KAGA near Jakobshavn Isbrae (JI), and KUAQ near Kangerdlugssuaq (KL); the station speeds reach 16.3 mm/a, 19.9 mm/a, and 18.7 mm/a, respectively. These fast-moving glaciers and the basin formed by Petermann Glacier (PG) account for approximately one-fifth of the Greenland ice sheet. For Jakobshavn Isbrae, the ice mass loss rate is (22±2) km^3/a, as observed by laser altimetry data in 2006–2009 (Khan et al., 2010), and this area's loss rate is still accelerating. For the Helheim and Kangerdluqssuaq Glaciers, the mass loss caused by dynamic changes in glaciers increased signific-

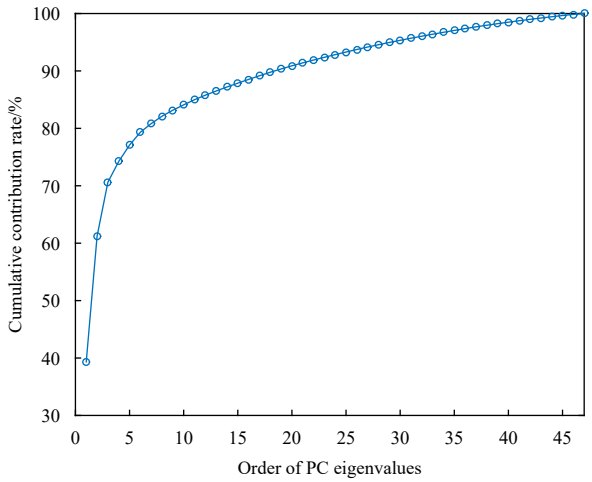

Fig. 2. Cumulative contribution rate of PC eigenvalues.

antly during 2005, and warm ocean and air temperatures further contributed to the thinning of glaciers (Khan et al., 2014). The velocities of stations in the northwest and northeast are relatively small, with an average speed of approximately 7.0 mm/a. The minimum vertical velocity occurs in the eastern region with an average of 3.4 mm/a, in which the speeds at the LBIB and HMBG are 3.2 mm/a and 2.8 mm/a, respectively. Overall, the velocity field of the GPS stations obtained in this paper is consistent with the results of Bevis et al. (2012) and Wake et al. (2016), although there are still differences for some stations. This difference is mainly because the data processing strategy is not exactly the same, and longer time series are used in this paper which can better cover the time span of tide gauge observations.

3.3 *Impact of current GrIS mass changes*

Accurate estimation of the vertical velocity caused by the current mass change in the Greenland ice sheet is significant for predicting global sea level change. To obtain the vertical deformation rate caused by the current ice and snow mass change, the impact of GIA should first be corrected. The separation of the elastic deformation rate and GIA rate can be achieved by using GIA models and differencing between GPS and gravity data (Nielsen et al., 2014; van Dam et al., 2007). Currently, the commonly used GIA global models mainly include ICE-3G (Tushingham and Peltier, 1991), ICE-4G (VM2) (Peltier, 1994), ICE-5G (VM2) (Peltier, 2004), ICE-6G_C (VM5a) (Peltier et al., 2015), ICE-4G+RF3L20 (β=0.4) (Wang et al., 2009, 2010), Paulson07 (Paulson et al., 2007), and the Geruo13 model (Geruo et al., 2012). The GIA models that show good performance in Greenland mainly include the GREEN1 model (Fleming and Lambeck, 2004), the Huy2 model (Simpson et al., 2009), and the Huy3 model (Lecavalier et al., 2014). Since the GRACE data in this paper used the Geruo13 model for GIA correction, the uplift rate of GPS stations is also corrected using this model.

The Geruo13 model is a global grid model with a resolution of 1°×1°. The cubic spline interpolation method is used to obtain the velocity field caused by GIA at the GPS station, as shown in Fig. 4. The overall GIA speed in Greenland is low, with an average of only 1.6 mm/a. However, the largest contribution to observed mass trends from GIA is in the north-east of Greenland with a maximum of 7.4 mm/a at LEFN station. This is also a region where there is a significant disagreement between different GIA models (Wake et al., 2016). Using the above velocity field to correct the GIA of the velocity field obtained by GPS observation, the vertical displacement velocity field caused by the current ice and snow mass change can be obtained. Due to the same GIA model used in GPS and GRACE data processing, the comparison between GPS and GRACE derived speed is more reasonable and convincing.

Figures 5 and 6 present the velocity fields of stations obtained by GPS, GIA and GRACE. The GIA-corrected vertical velocity of

Table 1. Comparison of residual stds before and after filtering at each station

Station name	Before filtering/mm	PCA filtering/mm	Improvement rate of std/%
ALRT	6.94	4.18	39.75
QAQ1	5.81	3.63	37.43
SCOR	6.13	4.11	32.98
THU3	6.70	3.67	45.16
KELY	6.11	3.97	35.07
asky	5.8	3.37	41.87
blas	6.70	3.54	47.22
dane	5.89	3.52	40.25
dgjg	5.21	3.11	40.40
dksg	5.90	3.30	44.05
gmma	6.48	3.63	43.92
grok	6.67	3.72	44.24
hel2	6.40	4.27	33.33
hjor	5.85	2.76	52.86
hmbg	4.81	2.79	41.87
hrdg	6.60	3.35	49.30
jgbl	6.72	4.02	40.17
jwlf	7.12	4.01	43.74
kaga	8.14	5.86	27.98
kagz	5.87	2.99	49.09
kbug	7.65	5.58	27.13
kmjp	6.91	4.12	40.42
kmor	6.90	3.84	44.31
ksnb	6.13	3.61	41.00
kuaq	5.98	3.56	40.48
kull	6.15	3.98	35.16
kulu	6.04	3.56	41.00
lbib	5.35	2.49	53.41
lefn	6.45	3.80	41.01
lyns	6.84	3.76	45.06
marg	6.32	3.63	42.58
mik2	5.94	3.55	40.23
msvg	5.93	3.43	42.08
nnvn	5.21	3.94	24.35
nrsk	6.61	4.29	35.07
plpk	6.54	3.95	39.58
qaar	6.25	5.11	18.26
rink	6.37	4.41	30.77
scby	6.76	4.87	28.04
senu	6.30	4.27	32.19
srmp	5.79	3.32	42.70
timm	7.23	4.41	38.99
treo	7.01	4.90	30.09
utmg	5.44	3.69	32.14
vfdg	5.59	3.48	37.80
wthg	5.64	2.71	52.03
ymer	6.16	3.35	45.63

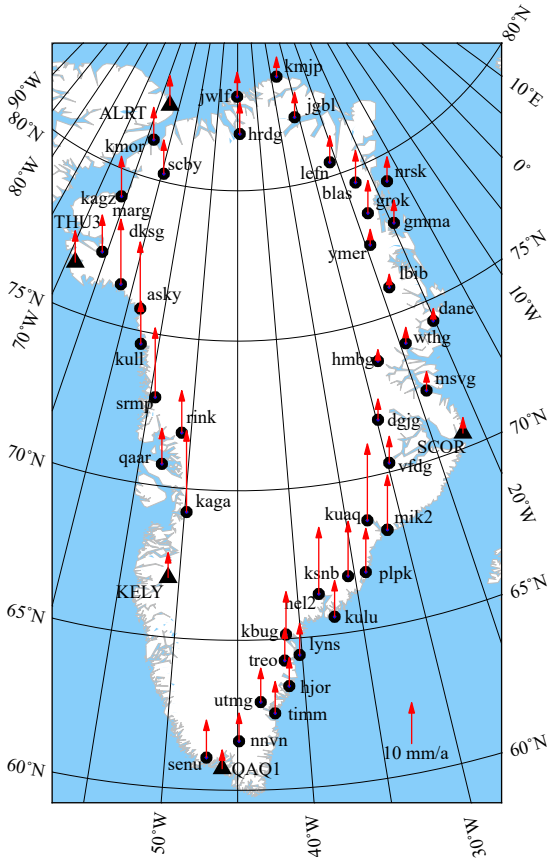

Fig. 3. GPS-based vertical velocity field in Greenland.

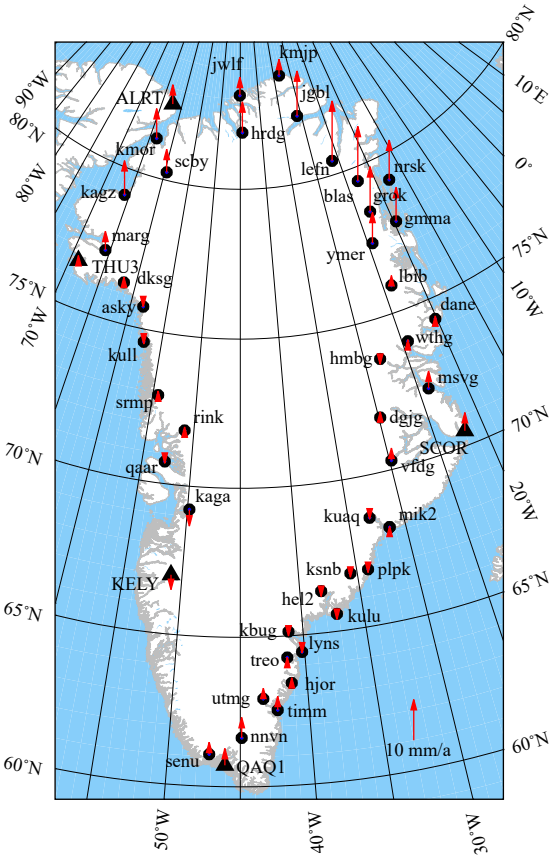

Fig. 4. The GIA-based speed field in Greenland.

the GPS is in good agreement with the vertical velocity obtained by GRACE, and the correlation coefficient is 0.7. However, there are also regional differences between the two kinds of velocities. For stations in the northeast (LEFN, YMER, JGBL, BLAS, and NRSK), the GIA-corrected speed of GPS and the speed of GRACE are in good agreement, so these stations are considered to be less affected by the current ice and snow mass changes. The stations in the east (DGJG, DANE, and WTHG) are less affected by GIA (less than 1.0 mm/a), and the GPS and GRACE speeds are also low. For stations in the southeast and west (KUAQ, MIK2, HEL2, KAGA, and SRMP), because their locations are close to outlet glaciers, the large mass loss of these outlet glaciers in recent years resulted in the higher speed, while the impact of GIA is small. The GPS results of these stations are quite different from the GRACE results because GRACE indicates large-scale mass movement, while GPS stations are sensitive to regional mass changes. In addition, Khan et al. (2016) pointed out that the impact of GIA in southeastern Greenland is underestimated. Stations in the south (QAQ1, SENU, TIMM, etc.) are also less affected by GIA (1.0–2.5 mm/a). The average vertical lifting speed caused by the ice and snow mass changes is 6.0–7.0 mm/a.

3.4 *Sea level change*

Figure 7 shows the monthly absolute sea level at NUUK, QAQO, SCOR, and THUL derived from the tide gauge stations and altimetric products of AVISO, where GPS-based vertical velocities at tide gauge stations were used to convert relative sea level

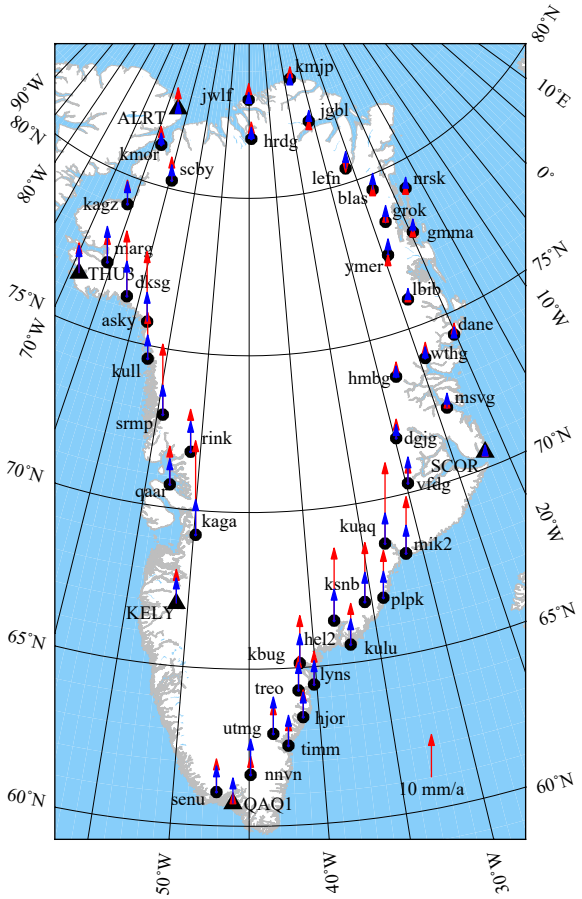

Fig. 5. GIA-corrected GPS speed field and GRACE speed field (red arrows represent GPS results, and blue arrows are GRACE results).

to absolute sea level. Except for NUUK, the other 3 tide gauge stations can provide observations for over 10 years, which is highly valuable for research on sea level change. Although the tide gauges show slightly higher sea level variability than the altimetry data, they have a good correlation with each other, except for THUL. For most areas of Arctic region, due to the presence of sea ice, it is difficult to derive the sea level from satellite altimetry in winter, especially in northwest Greenland, which means continuously operating tide gauge has unique advantages in monitoring sea level changes around Greenland.

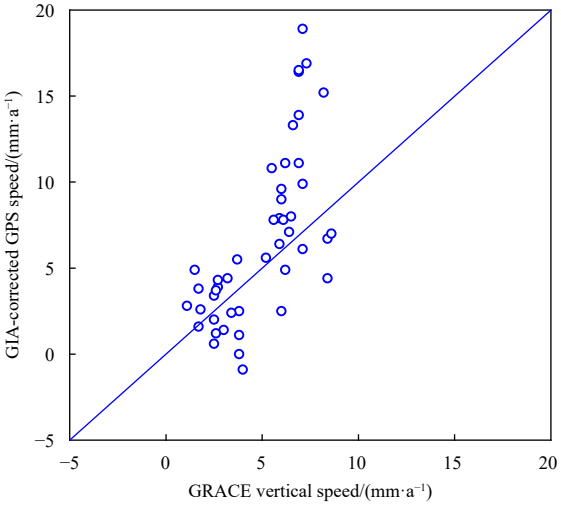

Fig. 6. Scatterplot of GIA-corrected GPS speed field and GRACE speed field.

Figures 8 and 9 show the absolute sea level trend at four tide gauge stations in Greenland. Due to vertical crustal movements in Greenland, it is necessary to convert relative sea level to absolute sea level by introducing GPS vertical velocity during the time span of tide gauge. In addition, it must be pointed out that the GPS vertical speed at NUUK is interpolated by inverse distance weighted due to the lack of NUUK GPS station in this paper. The monthly gridded products of absolute sea levels of AVISO were interpolated to the locations of tide gauges to better compare with tide gauge observations.

The GrIS holds 7.2 m of sea level equivalent and rising temperatures have led to accelerated mass loss in recent decades (Aschwanden et al., 2019), and an accumulated global sea level rise of 12 mm for GrIS from 1992 to 2016 was presented (Forsberg et al., 2017). However, regional eustatic movements along the coasts of Greenland are quite complex as shown in Figs 7–9. Notably, there is a dramatic decline in absolute sea level at THUL, which is located in northwest Greenland. Rose et al. (2019) also found a strong negative trend in northern Baffin Bay using radar altimetry. For SCOR and QAQO, the absolute sea level trend derived from tide gauge is also in good agreement with that from altimetry. Comparatively speaking, the sea level difference at NUUK derived from tide gauge and altimetry is non-ignorable. Spada et al. (2014) presented an inferred rate of sea level change of 1.9 mm/a at NUUK using tide gauge records from 1958 to 2002, however, it should be noted that the time period is different in this paper. Given the fact that only 4 years of NUUK

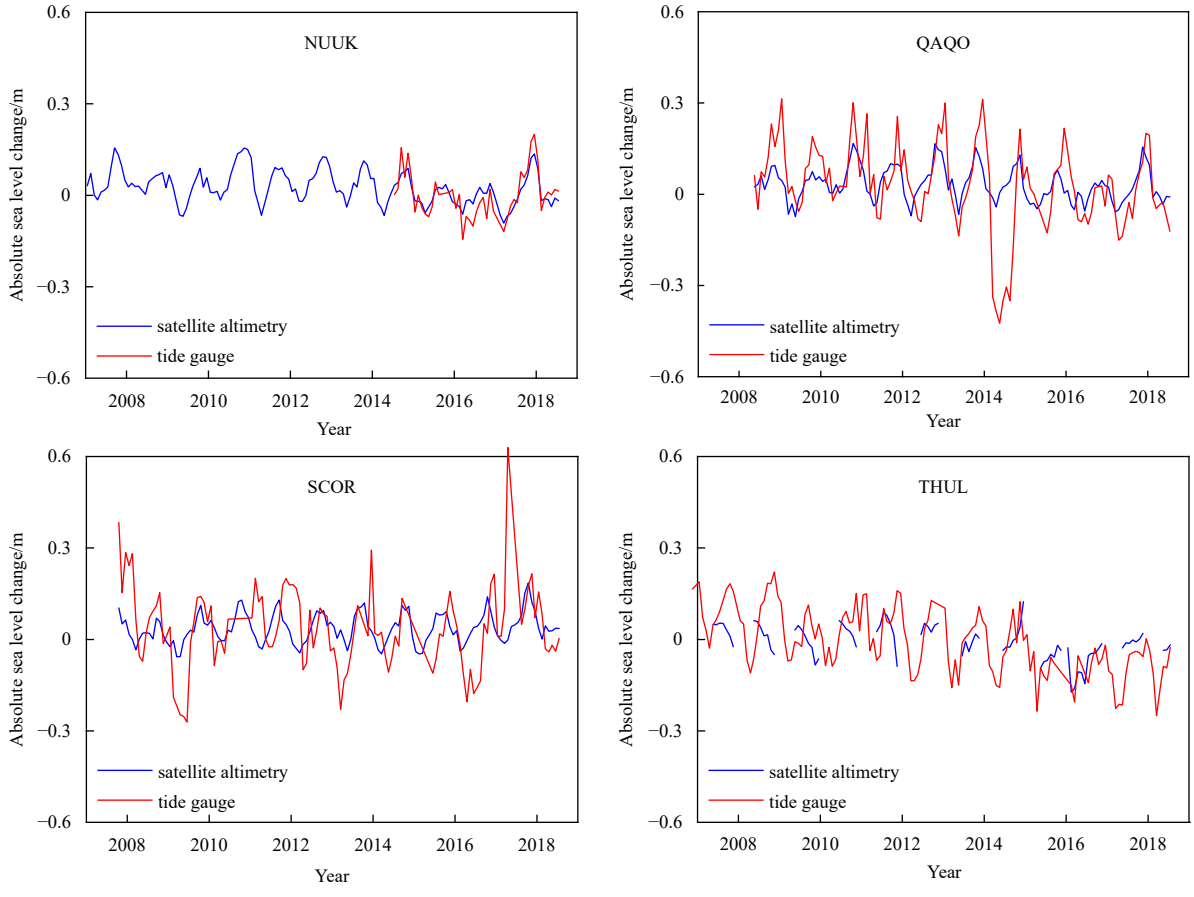

Fig. 7. Comparisons of monthly absolute sea level changes derived from tide gauge and satellite altimetry.

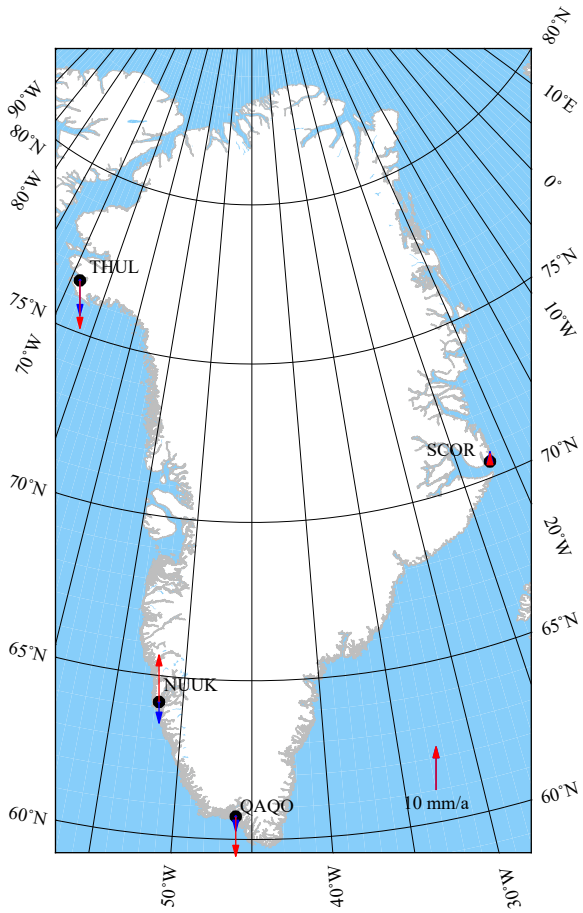

Fig. 8. Absolute sea level trends at four tide gauge stations in Greenland (red arrows represent absolute sea level trend derived from tide gauge, and blue arrows are sea level trend derived from satellite altimetry).

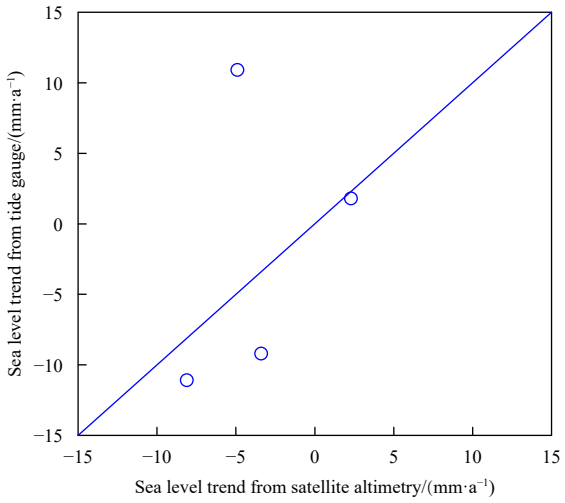

Fig. 9. Scatterplot of absolute sea level trends at four tide gauge stations in Greenland.

tide gauge observations are available and the good fit between tide gauge and satellite altimetry during the 4 years, the sea level fall at NUUK derived from satellite altimetry in 2007–2018 can be taken as a more reasonable result. Spada et al. (2012) found a pattern of regional sea level variations along the coasts of Greenland with measurements from ice cloud and land elevation satellite (ICESat) for the time period between 2003 and 2008, and argued that the regional sea level fall along the coasts of Greenland was strongly anticorrelated with vertical movements. This kind of anticorrelation can also be roughly found in Figs 5 and 8 at THUL, SCOR and QAQO. The fingerprints of sea-level rise is believed as the major driver of regional variations in sea levels (Hsu and Velicogna, 2017; Mitrovica et al., 2001). Sea level fingerprints (SLF) is characterized as changes of near-field sea level fall and far-field sea level rise in areas of intense ice mass loss such as Patagonia, coastal Alaska, the Amundsen Sea sector of West Antarctica, and the GrIS (Adhikari et al., 2019). By utilizing sea level observations from tide gauge stations and satellite altimetry, this research better illustrates the sea level changes in different coastal areas of Greenland, and can be further applied to the analysis of ice sheets and glaciers changes.

4 Conclusions

Global warming has caused dramatic ablation of the Greenland ice sheet, which means it is of importance to investigate vertical crustal movements and sea level change around Greenland. In this paper, the observations of more than 50 IGS and GNET GPS stations and tide gauge stations along the coast of Greenland are processed and analysed with other data sources such as satellite gravimetry, satellite altimetry and GIA. It is found that all GPS stations show an uplift trend, and the stations in southern Greenland have a higher vertical speed with a maximum of 20 mm/a, mainly because these stations are close to outlet glaciers. The influence of current GrIS mass changes is analysed, and it is shown that the GIA-corrected GPS velocity is consistent with the current glacier mass change model. By combining relative sea level from tide gauge records and crustal uplift rates derived from GPS observations, the absolute sea level around Greenland is obtained at 4 gauge stations, and validated using altimetric sea level products. Although the accelerated mass loss of GrIS can cause considerable global sea level rise, eustatic movements along the coasts of Greenland are quite complex under different mechanisms of sea level changes. Future works with more GPS and tide gauge stations and longer GPS and tide gauge observations can provide more accurate crustal uplift rates and sea level changes around Greenland.

Acknowledgements

We are grateful to IGS and UNAVCO for providing GPS observations, to DTU for sharing tide observations. Global gravity anomaly data were provided by JPL, and altimetric sea level anomaly products were obtained from AVISO.

References

Adhikari S, Ivins E R, Frederikse T, et al. 2019. Sea-level fingerprints emergent from GRACE mission data. Earth System Science Data, 11(2): 629–646, doi: 10.5194/essd-11-629-2019

Aschwanden A, Fahnestock M A, Truffer M, et al. 2019. Contribution of the greenland ice sheet to sea level over the next millennium. Science Advances, 5(6): eaav9396, doi: 10.1126/sciadv.aav9396

Bevis M, Wahr J, Khan S A, et al. 2012. Bedrock displacements in Greenland manifest ice mass variations, climate cycles and climate change. Proceedings of the National Academy of Sciences of the United States of America, 109(30): 11944–11948, doi: 10.1073/pnas.1204664109

Brunnabend S E, Schröter J, Rietbroek R, et al. 2015. Regional sea level change in response to ice mass loss in Greenland, the

West Antarctic and Alaska. Journal of Geophysical Research: Oceans, 120(11): 7316–7328, doi: 10.1002/2015JC011244
Chen Jianli, Wilson C R, Tapley B D. 2006. Satellite gravity measurements confirm accelerated melting of greenland ice sheet. Science, 313(5795): 1958–1960, doi: 10.1126/science.1129007
Cheng Yongcun, Andersen O, Knudsen P. 2015. An improved 20-year arctic ocean altimetric sea level data record. Marine Geodesy, 38(2): 146–162, doi: 10.1080/01490419.2014.954087
Cheng Minkang, Tapley B D, Ries J C. 2013. Deceleration in the Earth's oblateness. Journal of Geophysical Research: Solid Earth, 118(2): 740–747, doi: 10.1002/jgrb.50058
Dong Danan, Fang Peng, Bock Y, et al. 2006. Spatiotemporal filtering using principal component analysis and Karhunen-Loeve expansion approaches for regional GPS network analysis. Journal of Geophysical Research: Solid Earth, 111(B3): B03405
Fleming K, Lambeck K. 2004. Constraints on the Greenland Ice Sheet since the Last Glacial Maximum from sea-level observations and glacial-rebound models. Quaternary Science Reviews, 23(9–10): 1053–1077
Forsberg R, Sørensen L, Simonsen S. 2017. Greenland and antarctica ice sheet mass changes and effects on global sea level. Surveys in Geophysics, 38(1): 89–104, doi: 10.1007/s10712-016-9398-7
Geruo A, Wahr J, Zhong Shijie. 2012. Computations of the viscoelastic response of a 3-D compressible Earth to surface loading: An application to glacial isostatic adjustment in Antarctica and Canada. Geophysical Journal International, 192(2): 557–572
Herring T A, King R W, McClusky S C. 2015. Introduction to GAMIT/GLOBK (Release10.6). Cambridge, MA, USA: Massachusetts Institute of Technology, http://geoweb.mit.edu/gg/Intro_GG.pdf
Hsu C W, Velicogna I. 2017. Detection of sea level fingerprints derived from GRACE gravity data. Geophysical Research Letters, 44(17): 8953–8961, doi: 10.1002/2017GL074070
Khan S A, Kjeldsen K K, Kjaer K H, et al. 2014. Glacier dynamics at Helheim and Kangerdlugssuaq glaciers, southeast Greenland, since the Little Ice Age. The Cryosphere, 8(4): 1497–1507, doi: 10.5194/tc-8-1497-2014
Khan S A, Liu Lin, Wahr J, et al. 2010. GPS measurements of crustal uplift near Jakobshavn Isbræ due to glacial ice mass loss. Journal of Geophysical Research: Solid Earth, 115(B9): B09405
Khan S A, Sasgen I, Bevis M, et al. 2016. Geodetic measurements reveal similarities between post-Last Glacial Maximum and present-day mass loss from the Greenland ice sheet. Science Advances, 2(9): e1600931, doi: 10.1126/sciadv.1600931
Khan S A, Wahr J, Leuliette E, et al. 2008. Geodetic measurements of postglacial adjustments in Greenland. Journal of Geophysical Research: Solid Earth, 113(B2): B02402
Khan S A, Wahr J, Stearns L A, et al. 2007. Elastic uplift in southeast Greenland due to rapid ice mass loss. Geophysical Research Letters, 34(21): L21701, doi: 10.1029/2007GL031468
King M A, Altamimi Z, Boehm J, et al. 2010. Improved constraints on models of glacial isostatic adjustment: A review of the contribution of ground-based geodetic observations. Surveys in Geophysics, 31(5): 465–507, doi: 10.1007/s10712-010-9100-4
Lecavalier B S, Milne G A, Simpson M J R, et al. 2014. A model of Greenland ice sheet deglaciation constrained by observations of relative sea level and ice extent. Quaternary Science Reviews, 102: 54–84, doi: 10.1016/j.quascirev.2014.07.018
Li Juan, Zuo Juncheng, Chen Meixiang, et al. 2013. Assessing the global averaged sea-level budget from 2003 to 2010. Acta Oceanologica Sinica, 32(10): 16–23, doi: 10.1007/s13131-013-0361-x
Liu Lin, Khan S A, van Dam T, et al. 2017. Annual variations in GPS-measured vertical displacements near Upernavik Isstrøm (Greenland) and contributions from surface mass loading. Journal of Geophysical Research: Solid Earth, 122(1): 677–691, doi: 10.1002/2016JB013494
Mao Ailin, Harrison C G A, Dixon T H. 1999. Noise in GPS coordinate time series. Journal of Geophysical Research: Solid Earth, 104(B2): 2797–2816, doi: 10.1029/1998JB900033
Mitrovica J X, Tamisiea M E, Davis J L, et al. 2001. Recent mass balance of polar ice sheets inferred from patterns of global sea-level change. Nature, 409(6823): 1026–1029, doi: 10.1038/35059054
Nielsen E, Strykowski G, Forsberg R, et al. 2014. Estimation of PGR induced absolute gravity changes at greenland GNET stations. In: Rizos C, Willis P, eds. Earth on the Edge: Science for a Sustainable Planet. Berlin, Heidelberg: Springer
Paulson A, Zhong Shijie, Wahr J. 2007. Inference of mantle viscosity from GRACE and relative sea level data. Geophysical Journal International, 171(2): 497–508, doi: 10.1111/j.1365-246X.2007.03556.x
Peltier W R. 1994. Ice age paleotopography. Science, 265(5169): 195–201, doi: 10.1126/science.265.5169.195
Peltier W R. 2004. Global glacial isostasy and the surface of the ice-age earth: The ICE-5G (VM2) model and GRACE. Annual Review of Earth and Planetary Sciences, 32(1): 111–149, doi: 10.1146/annurev.earth.32.082503.144359
Peltier W R, Argus D F, Drummond R. 2015. Space geodesy constrains ice age terminal deglaciation: The global ICE-6G_C (VM5a) model. Journal of Geophysical Research: Solid Earth, 120(1): 450–487, doi: 10.1002/2014JB011176
Richter A, Rysgaard S, Dietrich R, et al. 2011. Coastal tides in West Greenland derived from tide gauge records. Ocean Dynamics, 61(1): 39–49, doi: 10.1007/s10236-010-0341-z
Rose S K, Andersen O B, Passaro M, et al. 2019. Arctic ocean sea level record from the complete radar altimetry era: 1991–2018. Remote Sensing, 11(14): 1672, doi: 10.3390/rs11141672
Simpson M J R, Milne G A, Huybrechts P, et al. 2009. Calibrating a glaciological model of the Greenland ice sheet from the Last Glacial Maximum to present-day using field observations of relative sea level and ice extent. Quaternary Science Reviews, 28(17–18): 1631–1657
Spada G, Galassi G, Olivieri M. 2014. A study of the longest tide gauge sea-level record in Greenland (Nuuk/Godthab, 1958–2002). Global and Planetary Change, 118: 42–51, doi: 10.1016/j.gloplacha.2014.04.001
Spada G, Ruggieri G, Sørensen L S, et al. 2012. Greenland uplift and regional sea level changes from ICESat observations and GIA modelling. Geophysical Journal International, 189(3): 1457–1474, doi: 10.1111/j.1365-246X.2012.05443.x
Swenson S, Chambers D, Wahr J. 2008. Estimating geocenter variations from a combination of GRACE and ocean model output. Journal of Geophysical Research: Solid Earth, 113(B8): B08410
Tapley B D, Bettadpur S, Watkins M, et al. 2004. The gravity recovery and climate experiment: Mission overview and early results. Geophysical Research Letters, 31(9): L09607
Tushingham A M, Peltier W R. 1991. Ice-3G: A new global model of Late Pleistocene deglaciation based upon geophysical predictions of post-glacial relative sea level change. Journal of Geophysical Research: Solid Earth, 96(B3): 4497–4523, doi: 10.1029/90JB01583
van den Broeke M R, Enderlin E M, Howat I M, et al. 2016. On the recent contribution of the Greenland ice sheet to sea level change. The Cryosphere, 10(5): 1933–1946, doi: 10.5194/tc-10-1933-2016
van Dam T, Wahr J, Lavallée D. 2007. A comparison of annual vertical crustal displacements from GPS and gravity recovery and climate experiment (GRACE) over Europe. Journal of Geophysical Research: Solid Earth, 112(B3): B03404
Wahr J, van Dam T, Larson K, et al. 2001. Geodetic measurements in Greenland and their implications. Journal of Geophysical Research: Solid Earth, 106(B8): 16567–16581, doi: 10.1029/2001JB000211
Wake L M, Lecavalier B S, Bevis M. 2016. Glacial isostatic adjustment (GIA) in Greenland: A review. Current Climate Change Reports, 2(3): 101–111, doi: 10.1007/s40641-016-0040-z
Wang Hansheng, Jia Lulu, Wu P, et al. 2010. Effects of global glacial isostatic adjustment on the secular changes of gravity and sea level in East Asia. Chinese Journal of Geophysics, 53(11): 2590–2602
Wang Hansheng, Wu P, van der Wal W, et al. 2009. Glacial isostatic

adjustment model constrained by geodetic measurements and relative sea level. Chinese Journal of Geophysics, 52(10): 2450–2460

Williams S D P, Bock Y, Fang Peng, et al. 2004. Error analysis of continuous GPS position time series. Journal of Geophysical Research: Solid Earth, 109(B3): B03412

Yang Qian, Wdowinski S, Dixon T H. 2013. Annual variation of coastal uplift in Greenland as an indicator of variable and accelerating ice mass loss. Geochemistry, Geophysics, Geosystems, 14(5): 1569–1589, doi: 10.1002/ggge.20089

Zhang Jie, Bock Y, Johnson H, et al. 1997. Southern California permanent GPS geodetic array: Error analysis of daily position estimates and site velocities. Journal of Geophysical Research: Solid Earth, 102(B8): 18035–18055, doi: 10.1029/97JB01380